CE: AK

INSTITUTE OF PHYSICS PUBLISHING WAVES IN RANDOM MEDIA

Waves Random Media **14** (2004) 1–13 PII: S0959-7174(04)79075-8

On the validity of some new acoustic scattering approximations

Subodh K Sharma[1] **and Ratan K Saha**[2]

[1] S N Bose National Centre for Basic Sciences, Block JD, Sector III, Salt Lake, Calcutta 700 098, India
[2] Saha Institute of Nuclear Physics, 1/AF, Bidhan Nagar, Calcutta 700 064, India

E-mail: sharma@bose.res.in

Received 12 April 2004
Published DD MMM 2004
Online at stacks.iop.org/WRM/14/1
doi:10.1088/0959-7174/14/0/000

Abstract

Two new approximations for predicting the elastic scattering of plane acoustic waves by a weak scatterer are proposed. The approximations have been obtained by drawing analogy between acoustic and light scattering problems. The validity of these approximations has been examined numerically for the exactly soluble case of scattering by a homogeneous sphere. Results show that for small angle scattering the proposed approximations have a considerably larger domain of validity in comparison to the extensively used Born approximation.

1. Introduction

In studies relating to the scattering of plane acoustic waves by an obstacle, exact analytic solutions are available only for certain simple shapes such as a long cylinder, a sphere, a disc, an ellipsoid etc. For scatterers of other shapes one needs to take resort to numerical solutions. A common approach, for example, is the T-matrix method [1]. However, the exact numerical solutions are highly computer intensive and provide little insight into the scattering processes involved. Besides, there are situations where even the numerical solutions are not possible. Thus, it is a common practice to employ approximation methods for describing the scattering processes.

The choice of approximation for a particular problem is generally governed by the characteristic size, d, and the acoustic properties of the scatterer. For example, if the scattering object is very small in comparison to the wavelength, λ, of the incident wave one may employ approximations like the long wavelength approximation and the Born approximation (BA) [2]. On the other hand, if the obstacle is much larger than the wavelength of the incident wave the diffraction approximation [2] may be used. The purpose of this paper is to describe two new approximations that predict accurately the elastic scattering of plane waves by an intermediate

size weak scatterer. The first approximation described in this paper is a modified form of the Born approximation (MBA), which extends the validity domain of the conventional BA to higher values of d. The second approximation, referred to as the eikonal approximation (EA), removes this restriction altogether but imposes a new condition, $\pi d/\lambda \gg 1$, for its validity if the scatterer is inhomogeneous. This requirement essentially means that the variation in scatterer density and compressibility over a wavelength is small. Similar approximations have been employed successfully in the context of electromagnetic wave scattering [3–6] and the potential scattering [6, 7]. But to the best of our knowledge, analogous approximations have not been derived or used in the context of acoustic scattering.

This paper is organized as follows. Section 2 contains basic formulae needed to describe the scattering of acoustic waves by an obstacle. In section 3 the expression for the scattering amplitude has been derived in framework of the MBA. For the particular case of a homogeneous spherical scatterer, for which exact solutions exist, the same result is rederived in section 4 starting from the exact analytic solutions. The alternative approach gives added insight into the validity of the MBA. The scattering amplitude in the EA has been derived in section 5. In section 6 these approximations have been validated numerically by comparing their predictions with exact results for the exactly soluble model of the scattering by a homogeneous spherical scatterer. Finally, section 7 contains summary of results and conclusions.

2. Basic definitions

The equation for the acoustic pressure p, either in the scattering region or outside, can be written in the form [2]

$$\nabla^2 p - \frac{1}{c^2}\frac{\partial^2 p}{\partial t^2} = \frac{1}{c^2}\frac{\partial^2 p}{\partial t^2}\gamma_\kappa(\mathbf{r}) + \operatorname{div}[\gamma_\rho(\mathbf{r})\operatorname{grad} p], \tag{1}$$

where

$$\gamma_\kappa(\mathbf{r}) = \frac{\kappa_e(\mathbf{r}) - \kappa}{\kappa} \qquad \gamma_\rho(\mathbf{r}) = \frac{\rho_e(\mathbf{r}) - \rho}{\rho_e(\mathbf{r})}, \tag{2}$$

inside the scattering region. Outside the scattering region $\gamma_\kappa = \gamma_\rho = 0$. Here κ and ρ are respectively the compressibility and the density of the medium surrounding the scatterer, κ_e and ρ_e are the corresponding quantities for the medium inside the scatterer and $c = 1/\sqrt{\rho\kappa}$ is the speed of the plane acoustic wave in the surrounding medium. Thus γ_κ and γ_ρ are measures of the mismatch of these quantities.

If the acoustic motion has a single frequency and the interaction is time independent, we may write $p = p_\omega \exp(-\mathrm{i}\omega t)$. The angle-distribution factor $\Phi_s(\theta)$, sometimes also referred to as the scattering amplitude may be expressed as [2]

$$\Phi_s(\theta) = \frac{k^2}{4\pi}\int\left[\gamma_\kappa(\mathbf{r}_0)p_\omega(\mathbf{r}_0) - \mathrm{i}\gamma_\rho(\mathbf{r}_0)\frac{\mathbf{a_r}}{k}\cdot\nabla_0 p_\omega(\mathbf{r}_0)\right]\exp(-\mathrm{i}\mathbf{k}_\mathrm{s}\cdot\mathbf{r}_0)\,\mathrm{d}\mathbf{r}_0, \tag{3}$$

where $\mathbf{a_r} = \mathbf{k}_\mathrm{s}/k$ is the unit vector in the direction of the observer and $\mathbf{r}_0$ is a point inside the scatterer volume. The scattering angle θ is the angle between the incident wave vector $\mathbf{k}$ and the final wave vector $\mathbf{k}_\mathrm{s}$. Since only the elastic scattering is of interest in this paper, $|\mathbf{k}| = |\mathbf{k}_\mathrm{s}| = k$. From (3) it is clear that if one knew the exact form of p_ω in the scattering region, one could compute the exact scattering amplitude. Thus the scattering problem under consideration reduces to finding p_ω inside the interaction region.

3. Modified Born approximation

Let us begin by defining a size parameter $x = \pi d/\lambda$ which can be looked upon as a convenient measure of the scatterer size in units of wavelength. Then if the inequalities

$$|\gamma_\kappa| \ll 1 \qquad |\gamma_\rho| \ll 1, \tag{4a}$$

$$x|\gamma_\kappa| < 1 \qquad x|\gamma_\rho| < 1, \tag{4b}$$

are satisfied, it may be assumed that the incident wave is not greatly disturbed by the scatterer. That is the pressure field inside the scatterer may be taken to be the same as the incident pressure field. Thus for an incident plane wave one may approximate

$$p_\omega(\mathbf{r}_0) = \exp(\mathrm{i}\mathbf{k}\cdot\mathbf{r}_0). \tag{5}$$

This is nothing but the BA. The conditions (4*a*) imply that the BA is valid whenever the mismatch between the acoustic properties of the medium and the scatterer is small. Such a scatterer may be termed a weak scatterer. The inequalities (4*b*) mean that the phase change in the incident wave is negligible. The inequality also governs the maximum value of d for which the BA is expected to yield good results.

The angle distribution factor in the BA can be obtained by substituting (5) in (3). This gives [2]

$$\Phi_b(\theta) = \frac{k^2}{4\pi}\int [\gamma_\kappa(\mathbf{r}_0) + \gamma_\rho(\mathbf{r}_0)\cos\theta]\exp(\mathrm{i}\mathbf{q}\cdot\mathbf{r}_0)\,\mathrm{d}\mathbf{r}_0, \tag{6}$$

where $\cos\theta = \mathbf{k}\cdot\mathbf{k}_\mathrm{s}/k^2$ is the cosine of the angle between the direction of the incident plane wave and the direction of the observer, $\mathbf{q} = \mathbf{k} - \mathbf{k}_\mathrm{s}$ is the difference of the incident and final wave vectors whose magnitude is $q = 2k\sin(\theta/2)$. The subscript b refers to the BA. For the particular case of scattering by a homogeneous sphere, the integration in (5) can be performed analytically to yield

$$\Phi_b(\theta) = \frac{x^2}{q}[\gamma_\kappa + \gamma_\rho\cos\theta]j_1(qa), \tag{7}$$

where a is the radius of the sphere and $j_1(qa)$ is the spherical Bessel function of order unity. It may be noted here that if γ_κ and γ_ρ are real, the scattered intensity $i_b(\theta) = |\phi_b(\theta)|^2$ becomes zero whenever $\gamma_\kappa + \gamma_\rho\cos\theta = 0$.

For a very small particle ($a \to 0$) one may approximate $j_1(qa) \cong qa/3$. This gives

$$\Phi_b(\theta) \approx \frac{x^3}{3k}[\gamma_\kappa + \gamma_\rho\cos\theta], \tag{8}$$

which may be contrasted with

$$\Phi_l(\theta) = \frac{x^3}{3k}\left[\gamma_\kappa + \frac{3\rho_e - 3\rho}{2\rho_e + \rho}\cos\theta\right], \tag{9}$$

which is the angle-distribution factor in the long wavelength limit [2]. If $\rho_e \approx \rho$, (8) and (9) are approximately equal.

Saxon [3], in the context of electromagnetic scattering, has suggested a modified BA in which the wave vector of the incident wave is modified by a multiplicative factor k_e/k inside the interaction region. This allows the properties of the scatterer to enter the BA. Shimizu [4] has tested the predictions of this approximation for scattering by a homogeneous dielectric sphere. It was found that the angular positions of successive extrema in the scattering pattern could be reproduced much more accurately in the MBA. The findings were confirmed by

Sharma and Somerford [8] for the scattering of electromagnetic waves by an infinitely long cylinder. Drawing an analogy with electromagnetic case, we approximate

$$p_\omega(\mathbf{r}_0) = \exp(in\mathbf{k}\cdot\mathbf{r}_0),$$

where $n = k_e/k$. When substituted in (3) this leads to

$$\Phi_{\rm mb}(\theta) = \frac{k^2}{4\pi}\int [\gamma_\kappa(\mathbf{r}_0) + n\gamma_\rho(\mathbf{r}_0)\cos\theta]\exp(\mathrm{i}\mathbf{R}\cdot\mathbf{r}_0)\,\mathrm{d}\mathbf{r}_0, \tag{10}$$

where $\mathbf{R} = n\mathbf{k} - \mathbf{k}_{\rm s}$ and the subscript mb stands for the MBA. For a homogeneous sphere the integration in (10) is straightforward. One obtains

$$\Phi_{\rm mb}(\mathbf{k}_{\rm s}) = \frac{x^2}{R}[\gamma_\kappa + n\gamma_\rho\cos\theta]j_1(Ra), \tag{11}$$

where $R = k\sqrt{1+n^2-2n\cos\theta}$. Theoretically, the validity domain of this approximation is same as that of the BA. To examine their relative accuracy one must take resort to numerical comparisons. This has been done in section 6 where the predictions of approximations have been compared with exact results in the framework of exactly soluble model of scattering by a homogeneous sphere.

4. Alternative derivation: the S-approximation

For a homogeneous sphere the exact scattering amplitude using the partial wave expansion can be written as [2]

$$\Phi(\theta) = \frac{\mathrm{i}}{k}\sum_m (2m+1)b_m P_m(\cos\theta), \tag{12}$$

where

$$b_m = \frac{j_m'(x)j_m(y) - \alpha j_m(x)j_m'(y)}{h_m'(x)j_m(y) - \alpha h_m(x)j_m'(y)}, \tag{13}$$

with $x = ka$, $y = nx$, $n = k_e/k = c/c_e$, $\alpha = n\rho/\rho_e$ and primes signify the differentiation with respect to the argument. The spherical Hankel function is defined as $h_m(x) = j_m(x) + \mathrm{i}n_m(x)$ with j_m and n_m as the spherical Bessel and the spherical Neumann functions of order m respectively. The parameter α is related to acoustic impedances of scatterer (Z_e) and the acoustic impedance of the medium (Z) via the relation $\alpha = Z/Z_e$. Alternatively, this may also be written as $\alpha = n(1-\gamma_\rho)$.

In the limit, $\alpha \to 1$ and $n \to 1$, the denominator in (13) can be approximated as [10]

$$h_m'(x)j_m(x) - h_m(x)j_m'(x) = \frac{\mathrm{i}}{x^2}, \tag{14}$$

allowing one to write

$$b_m = -\mathrm{i}x^2\left[\frac{\partial F}{\partial x} - \alpha\frac{\partial F}{\partial y}\right], \tag{15}$$

where $F = j_m(x)j_m(y)$. The infinite series (12) can then be summed using the relation [10]

$$\sum_{m=0}^{\infty}(2m+1)\,j_m(x)j_m(y)P_m(\cos\theta) = \frac{\sin(xR)}{xR},$$

yielding

$$\Phi_s(\theta) = \frac{x^2}{R}[\gamma_\kappa + n\gamma_\rho\cos\theta]j_1(Ra). \tag{16}$$

It is interesting to note that the scattering amplitude (16) is identical with (11). In optics, the corresponding approximation is known as the S-approximation [5, 6]. Hence the subscript s. The assumptions $n \to 1$ and $\alpha \to 1$ imply ρ_e/ρ as well as κ_e/κ to be close to unity. Note that in this derivation apparently no restriction has been placed either on the size of the scatterer or on the angular range of the approximation. However, it should be recognized that while approximating the denominator in (13) by (14) one is also neglecting terms involving x and θ. We shall see later, in numerical comparisons, that this approximation is indeed valid only for a restricted domain of x and θ values.

5. The eikonal approximation

The EA has been extensively used in problems relating to light scattering by obstacles whose relative refractive index is close to unity [6, 11]. In optics, this approximation has been implemented in a number of ways. It may be introduced either in the differential equation or in the corresponding integral equation or at the level of Green's function. Each approach brings out a different feature of the approximation more clearly. Here, the approximation has been introduced in the differential equation (1). It is assumed that for a weak scatterer a plausible solution of (1) may be written as

$$p_\omega(\mathbf{r}) = \exp(\mathrm{i}kz)\phi(\mathbf{b}, z) \tag{17}$$

where $\phi(\mathbf{b}, z)$ is a slowly varying function of position. Without any loss of generality the z-axis may be chosen along the incident wave vector direction. The vector $\mathbf{b}$ is the impact parameter vector in the two-dimensional space transverse to z. Substitution of p_ω from (17) in (1) then gives

$$(1-\gamma_\rho(\mathbf{r}))\nabla^2\phi(\mathbf{b}, z) + 2\mathrm{i}k(1-\gamma_\rho(\mathbf{r}))\frac{\partial\phi(\mathbf{b}, z)}{\partial z} + k^2(1+\gamma_\kappa(\mathbf{r}))\phi(\mathbf{b}, z)$$
$$-k^2(1-\gamma_\rho(\mathbf{r}))\phi(\mathbf{b}, z) = \mathrm{i}k\phi(\mathbf{r})\frac{\partial}{\partial z}\gamma_\rho(\mathbf{r}) + \nabla\gamma_\rho(\mathbf{r})\cdot\nabla\phi(\mathbf{r}), \tag{18}$$

which may also be recast as

$$\left[\nabla^2 + 2\mathrm{i}k\frac{\partial}{\partial z}\right]\phi(\mathbf{b}, z) + \frac{k^2[\gamma_\kappa(\mathbf{r})+\gamma_\rho(\mathbf{r})]}{1-\gamma_\rho(\mathbf{r})}\phi(\mathbf{b}, z) = \frac{\mathrm{i}k\phi(\mathbf{r})[\partial\gamma_\rho(\mathbf{r})/\partial z] + \nabla\gamma_\rho(\mathbf{r})\cdot\nabla\phi(\mathbf{r})}{1-\gamma_\rho(\mathbf{r})}. \tag{19}$$

The EA consists in neglecting ∇^2 term in (19). In addition the right-hand side is also set equal to zero here. This is justified because both $\phi(\mathbf{r})$ and $\gamma_\rho(\mathbf{r})$ are assumed to be slowly varying functions in space. This leads to the following equation

$$\frac{\partial\phi(\mathbf{b}, z)}{\partial z} = \frac{k}{2\mathrm{i}}[1-n^2(\mathbf{r})]\phi(\mathbf{b}, z). \tag{20}$$

The neglect of ∇^2 term amounts to conditions [6, 11]

$$|1-n^2(\mathbf{r})| \ll 1 \qquad ka \gg 1.$$

The condition $ka \gg 1$ basically arises from the requirement that the variation in the scattering properties of the scatterer over a wavelength is small. It is apparent that for a homogeneous scatterer this condition is redundant. This condition also justifies the neglect of right-hand side term in (19). For a homogeneous scatterer $\nabla\gamma_\rho$ inside the scatterer is zero anyway. It has been assumed that the mathematical difficulties arising due to sharp cut-off at the boundaries of the scatterer are not relevant physically. The validity of this assumption has been amply verified in light scattering problems [6, 11].

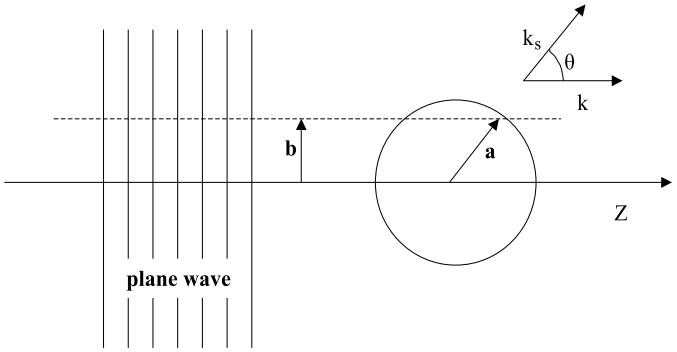

Figure 1. Scattering of a plane wave by a scatterer in the eikonal approximation.

The solution of (20) is straightforward. Employing the boundary condition that $\phi(\mathbf{b}, z) = 1$ at $z = -\infty$, one can write

$$\phi(\mathbf{r}) = \exp\left(\frac{k}{2\mathrm{i}}\int_{-\infty}^{z}[1 - n^2(\mathbf{b}, z')]\,\mathrm{d}z'\right), \tag{21}$$

leading to

$$p_\omega(\mathbf{r}) = \exp\left(\mathrm{i}kz + \frac{k}{2\mathrm{i}}\int_{-\infty}^{z}[1 - n^2(\mathbf{b}, z')]\,\mathrm{d}z'\right). \tag{22}$$

This is the pressure field inside the scatterer in the EA. The physical picture that emerges from this solution is as follows. A plane wave is assumed to pass through the scattering particle at an impact parameter b in a straight line trajectory as shown in figure 1. The presence of the scatterer introduces a change in the phase of the incident wave. Its amplitude remains unaffected.

The scattering amplitude is obtained by substituting (22) into (3). If one is interested in either near forward or near backward scattering, $\mathbf{a_r} \cdot \boldsymbol{\nabla}_0$ may be approximated by $\cos\theta \frac{\partial}{\partial z_0}$. The terms neglected are of the order $\theta(1 - n^2)$. The scattering amplitude may thus be written as

$$\Phi_{\mathrm{eik}}(\theta) = \frac{k^2}{4\pi}\int \mathrm{d}^2 b_0\,\mathrm{d}z_0\left[\gamma_\kappa(\mathbf{r}_0) + \frac{[1 + n^2(\mathbf{r}_0)]\cos\theta}{2}\gamma_\rho(\mathbf{r}_0)\right]$$
$$\times \exp(\mathrm{i}q_z z_0)\exp(\mathrm{i}\mathbf{q}_\perp \cdot \mathbf{b_0})\exp\left(\frac{-\mathrm{i}k}{2}\int_{-\infty}^{z_0}[1 - n^2(\mathbf{b}_0, z)]\,\mathrm{d}z\right), \tag{23}$$

where $q_z = 2k\sin^2(\theta/2)$ and $q_\perp = k\sin\theta$. For a spherically symmetric scatterer, the integration over azimuthal angle may be performed using the relation

$$\frac{1}{2\pi}\int_0^{2\pi}\mathrm{d}\phi\exp(\mathrm{i}qb\cos\phi) = J_0(qb)$$

to yield

$$\Phi_{\mathrm{eik}}(\theta) = \frac{k^2}{2}\int b_0\,\mathrm{d}b_0\,\mathrm{d}z_0\left[\gamma_\kappa(b_0, z_0) + \frac{[1 + n^2(b_0, z_0)]\cos\theta}{2}\gamma_\rho(b_0, z_0)\right]J_0(q_\perp b_0)$$
$$\times \exp(\mathrm{i}q_z z_0)\exp\left(\frac{-\mathrm{i}k}{2}\int_{-\infty}^{z_0}[1 - n^2(b_0, z)]\,\mathrm{d}z\right) \tag{24}$$

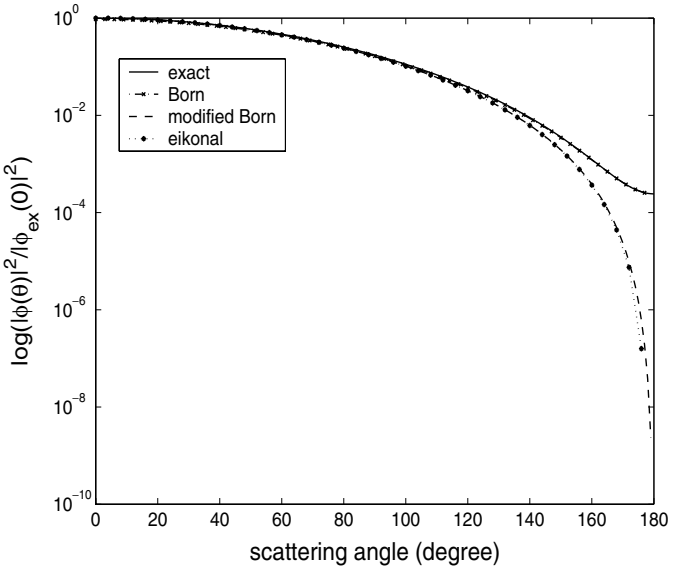

Figure 2. Angular scattering pattern of various approximations compared against exact partial wave results. In this figure $x = 1.0$ and $\rho_e/\rho = \kappa_e/\kappa = 1.05$. The y-axis is base 10 logarithmic scale.

which is a simple two-dimensional integral representation of the scattering amplitude. The straight line propagation obtained in the EA clearly implies that it is a small angle approximation. Indeed a detailed examination of the angular validity domain of the EA shows [6, 7] that $\theta \ll 1/\sqrt{x}$ if $|x(1-n^2)| < 1$ or $\theta \ll |1-n^2|^{1/2}$ if $|x(1-n^2)| > 1$.

For the special case of a homogeneous spherical scatterer, the z integration in equation (24) can be performed yielding the one-dimensional impact parameter representation of the scattering amplitude

$$\Phi_{\mathrm{eik}}(\theta) = \frac{k^2}{\mu}\left[\gamma_\kappa + \frac{(1+n^2)\cos\theta}{2}\gamma_\rho\right]\int_0^a b_0\,\mathrm{d}b_0\,J_0(q_\perp b_0) \times \sin\left(\mu\sqrt{(a^2-b_0^2)}\right)\exp\left(\frac{-\mathrm{i}k}{2}(1-n^2)\sqrt{(a^2-b_0^2)}\right), \tag{25}$$

where $\mu = q_z - \frac{k}{2}(1-n^2)$. For forward scattering, the integration in (25) can be carried out analytically and one obtains

$$\Phi_{\mathrm{eik}}(0) = \frac{\mathrm{i}x^2}{(n^2-1)k}\left(\gamma_\kappa + \frac{(1+n^2)}{2}\gamma_\rho\right)\left[\frac{1}{2} + \frac{\mathrm{i}\mathrm{e}^{\mathrm{i}\beta}}{\beta} - \frac{\mathrm{e}^{\mathrm{i}\beta}-1}{\beta^2}\right] \tag{26}$$

where $\beta = ka(n^2-1)$. The integration can be done analytically for backscattering also. It may be mentioned here that a number of variants of the EA have been employed in the context of potential scattering [6] and in the optical scattering [6, 12]. The variant of the EA used here has been adapted from Perrin and Chiapetta [12]. This variant is known to be a better approximation in reproducing the positions of maxima and minima more accurately compared to other versions [12].

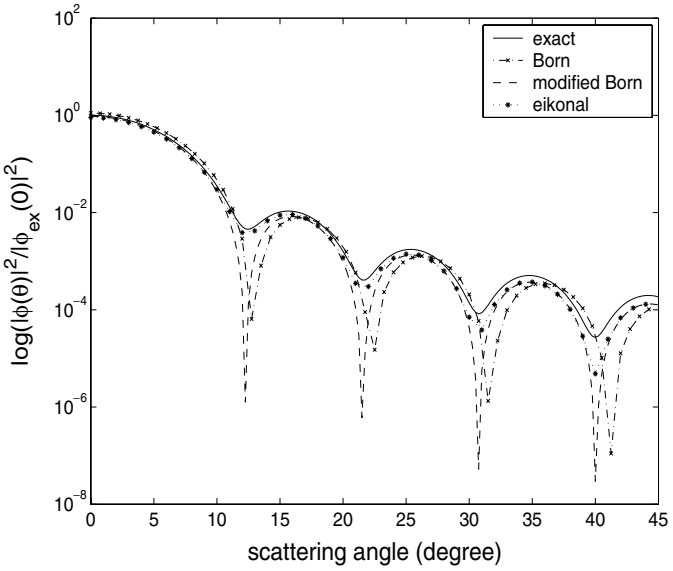

Figure 3. Angular scattering pattern of various approximations compared against exact partial wave results. In this figure $x = 20.0$ and $\rho_e/\rho = \kappa_e/\kappa = 1.05$. The y-axis is base 10 logarithmic scale.

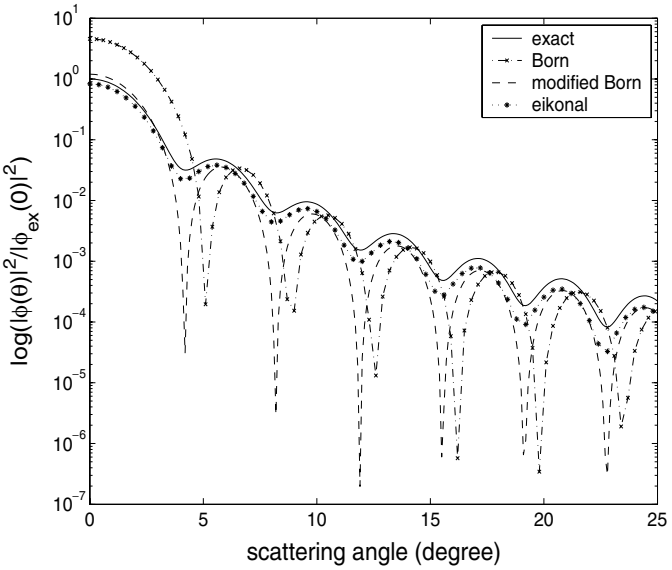

Figure 4. Angular scattering pattern of various approximations compared against exact partial wave results. In this figure $x = 50.0$ and $\rho_e/\rho = \kappa_e/\kappa = 1.05$. The y-axis is base 10 logarithmic scale.

In the limit $x|n-1| \ll 1$, the expansion of the exponential term in (25) gives the leading term,

$$\Phi_{\rm eik}(\theta) \approx \frac{a}{\mu^2}\left[\gamma_\kappa + \frac{n^2+1}{2}\gamma_\rho \cos\theta\right] j_1(qa) \tag{27}$$

which in the limit $n \to 1$ is the BA (7).

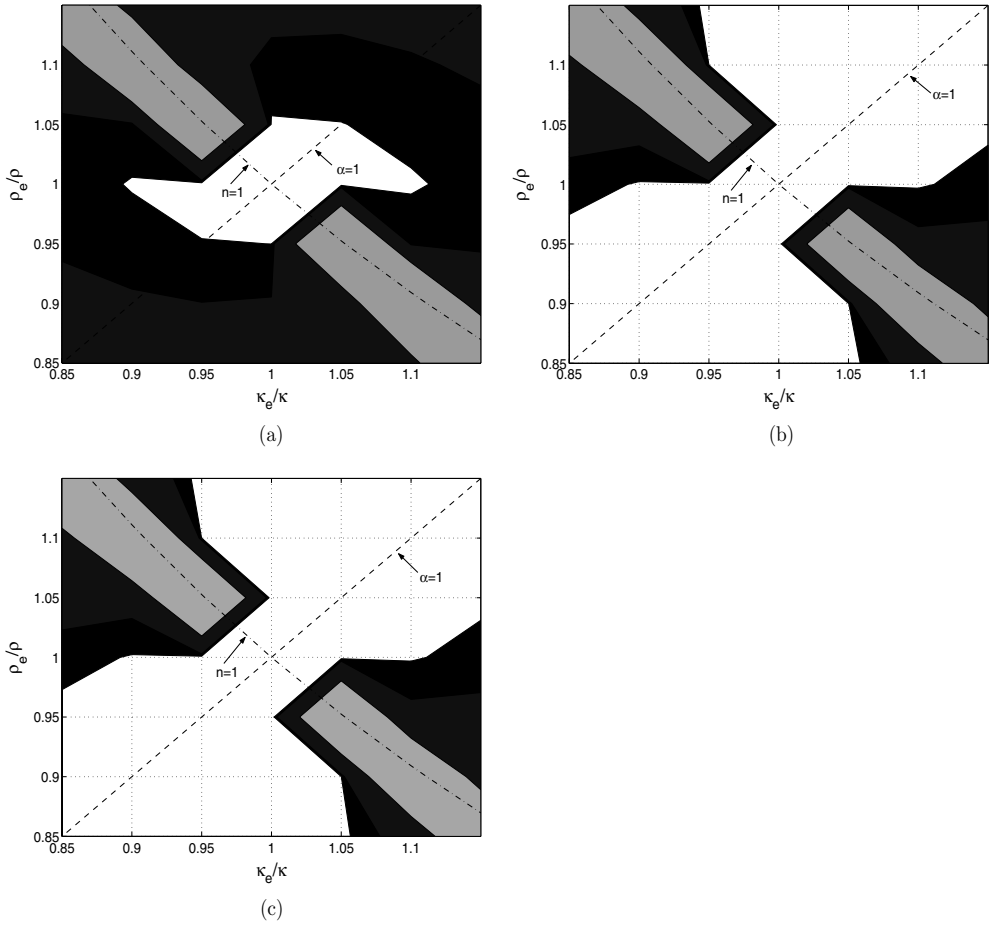

Figure 5. (a) Forward scattering error contour chart for $x = 1.0$ in the BA. White area: error $<$ 5%; darkest area: error $<$ 10%; less dark area: error $<$ 50% and least dark area: error $>$ 50%. (b) Same as (a) but for the MBA. (c) Same as (a) but for the EA.

6. Numerical comparisons

This section examines the validity domains of the BA, the MBA and the EA numerically by comparing them against the exact results for the scattering of plane acoustic waves by a homogeneous sphere. The exact results have been obtained by computing (12).

Figures 2, 3 and 4 compare normalized angular scattering functions, $|\Phi(\theta)|^2/|\Phi_{\rm ex}(0)|^2$, in various approximations with exact angular scattering functions for $x = 1.0$, $x = 20.0$ and $x = 50.0$ respectively. The plots are for $|\Phi(\theta)|^2/|\Phi_{\rm ex}(0)|^2$. The value of $\kappa_e/\kappa = \rho_e/\rho = 1.05$ in these figures. It can be seen from figure 2 that for small obstacles all three approximations are equally good in predicting scattered intensity over almost entire range of scattering angles. Predictions differ at backward angles. The BA is distinctly better than other approximations at backward angles. The MBA and the EA are nearly identical throughout the angular domain. The angular range over which approximations are valid reduces with increasing x. This can be seen in figure 3 where angular scattering patterns for $x = 20.0$ are shown. The BA here is distinctly inferior to the MBA and the EA. In particular, the positions of minima and maxima

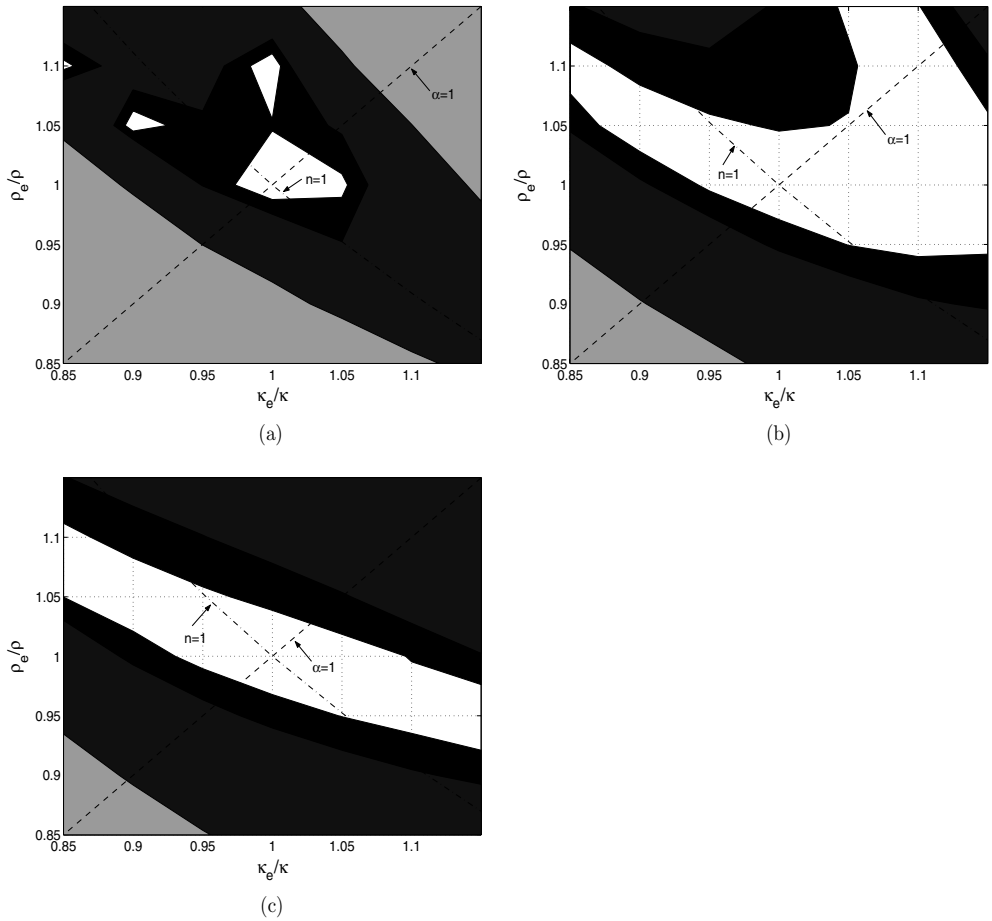

Figure 6. (a) Forward scattering error contour chart for $x = 20.0$ in the BA. White area: error $<$ 5%; darkest area: error $<$ 10%; less dark area: error $<$ 50% and least dark area: error $>$ 50%. (b) Same as (a) but for the MBA. (c) Same as (a) but for the EA.

are very accurately reproduced in the EA and the MBA. This observation is important because the positions of maxima and minima can potentially be used to predict the size of the scatterer employing the MBA [4, 7]. The EA also reproduces the depth of the positions of minima reasonably well while the MBA fails to do that. The BA is inferior to other approximations even in the forward direction. The conclusions drawn from figure 3 become more apparent in figure 4 where the angular scattering patterns are plotted for $x = 50.0$. None of the approximations reproduce large angle scattering pattern very well.

For examining the validity of these approximations in the $(\gamma_\kappa, \gamma_\rho)$ domain, it is useful to define per cent error in approximations as

$$\text{per cent error} = \frac{[|\Phi_{\text{ex}}(0)|^2 - |\Phi_{\text{appx}}(0)|^2] \times 100}{|\Phi_{\text{ex}}(0)|^2}.$$

Since the MBA and the EA are small angle approximations, a natural choice for scattering angle in these comparisons is $\theta = 0$. The error contour charts for various approximations are shown in figures 5, 6 and 7 for $x = 1.0, x = 20.0$ and $x = 50.0$ respectively. The values of ρ_e/ρ and κ_e/κ have been varied in the domain 0.85–1.15. Figures 5(a)–(c) show the error

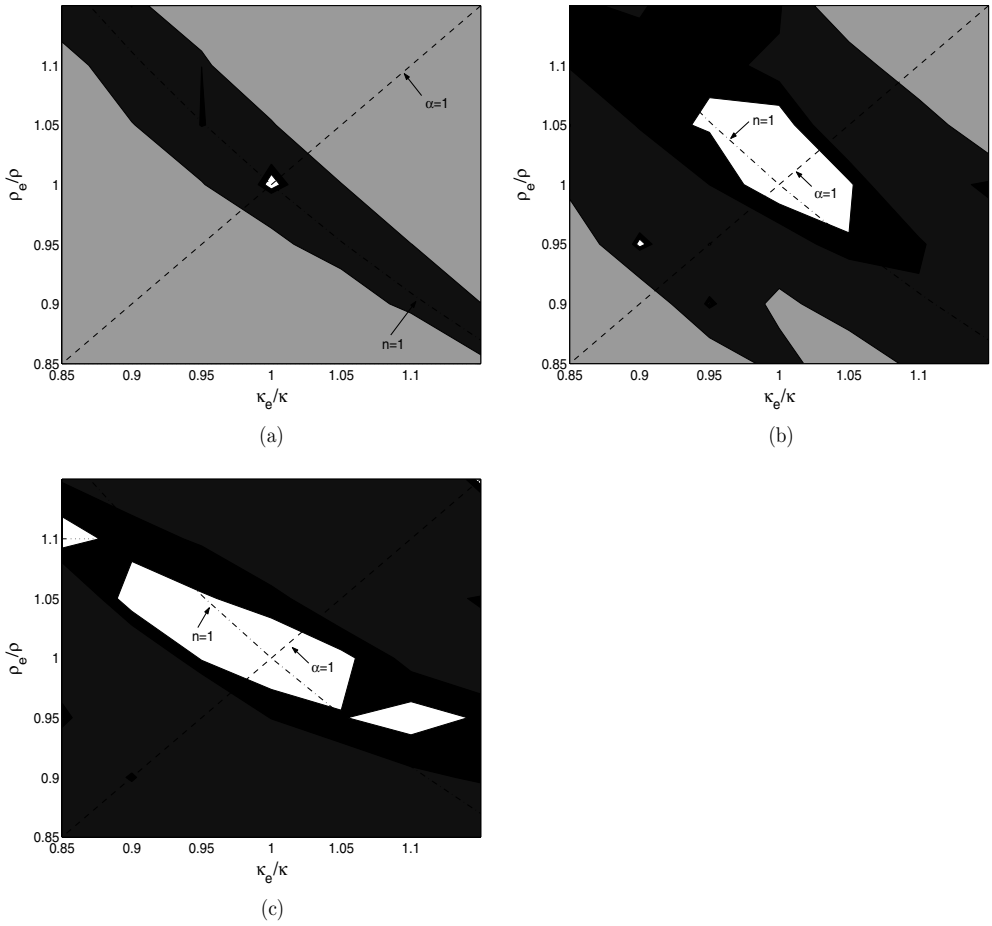

Figure 7. (a) Forward scattering error contour chart for $x = 50.0$ in the BA. White area: error $<$ 5%; darkest area: error $<$ 10%; less dark area: error $<$ 50% and least dark area: error $>$ 50%. (b) Same as (a) but for the MBA. (c) Same as (a) but for the EA.

contour charts for the three approximations when $x = 1$. It is clear from these figures that while the BA is a good approximation over a large $(\gamma_\kappa, \gamma_\rho)$ domain, the EA and the MBA have far enlarged validity domain. The area covering errors less than 5% is much greater for the MBA and the EA in comparison to the BA. The error contour charts for the EA and the MBA may be noted to be nearly identical for this case. The line joining the coordinates (0.85, 0.85) and (1.15, 1.15) is the line $\alpha = 1$. Clearly the approximations should be viewed as $\alpha \to 1$ approximations. Note that the errors can become quite large even if n is close to unity but if α is not close to unity. Figures 6(a)–(c) depict the error contour charts for $x = 20.0$. It can be seen that the domain over which the BA gives good results has shrunk considerably. It may be noted again that the validity domains of the MBA and the EA are much larger in comparison to that of the BA. The errors in the EA are less than 50% over the entire domain examined. On the other hand, domain where the errors are less than 10% is larger for the MBA in comparison to the EA. Figures 7(a)–(c) show plots of error contour charts for various approximations for large scatterers ($x = 50.0$). The errors in the BA are very large. The EA is distinctly the best approximation for large scatterers.

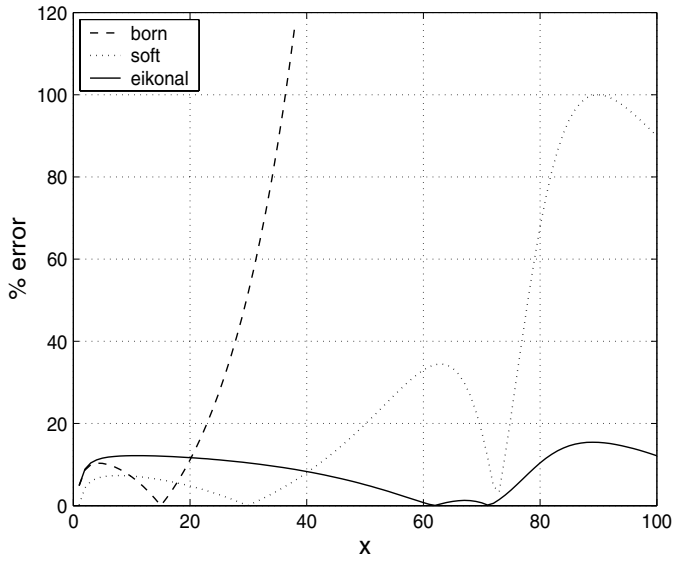

Figure 8. The per cent error in the forward scattering as a function of x for various approximations. Here $\kappa_e/\kappa = \rho_e/\rho = 1.05$.

Figure 8 shows per cent error as a function of size parameter x for a typical weak scatterer. The scattering angle chosen in this comparison is $\theta = 0$. It is clear from the figure that for a weak scatterer the EA is indeed the most useful approximation for forward scattering angles.

7. Conclusions

This paper considers scattering of plane acoustic waves by a weak scatterer in the intermediate size range. This range is generally recognized as the most difficult regime for scattering calculations. Two approximations suitable for near forward scattering in this regime have been derived by drawing an analogy with the scattering of electromagnetic waves by an obstacle. The approximations are (i) the modified Born approximation and (ii) the eikonal approximation. These approximations are expected to find wide use in the analysis of acoustic scattering in various contexts.

The validity of the BA, the MBA and the EA has been examined numerically for the exactly soluble problem of acoustic wave scattering by a weakly scattering homogeneous sphere. Following conclusions may be drawn from these comparisons. (i) The MBA and the EA are very useful approximations for weak scatterers in the intermediate size domain for predicting small angle scattering. The MBA greatly increases the validity domain of the conventional BA without destroying the simplicity of the BA. Thus, the MBA can be used in most problems in place of the conventional BA with enhanced accuracy. (ii) The validity of the EA is not limited to intermediate size particles only. For a homogeneous scatterer, this approximation does not place any restriction on the size of the scatterer. For an inhomogeneous scatterer its validity requires $x \gg 1$. This arises from the requirement of slow variation of $\gamma_\kappa(\mathbf{r})$ and $\gamma_\rho(\mathbf{r})$ in space. But despite the theoretical requirement $x \gg 1$, the approximation is known to work well for small particles too because in this limit it reduces to the BA for weak scatterers. The maximum error in the range $x < 100$ in forward scattered intensity is about 20% for $\kappa_e/\kappa = \rho_e/\rho = 1.05$ which is much less in comparison to other approximations.

(iii) For small particles $x < 1$, the BA is the most suitable approximation for backward scattering. For forward scattering, the MBA and the EA have a larger validity domain in terms of ρ_e/ρ and κ_e/κ.

It was pointed out in section 6 that the positions of maxima and minima in the scattering pattern are reproduced very accurately by the MBA and the EA. Since the positions of maxima and minima in the angular scattering pattern are related to the size of the scatterer via zeros of the Bessel function $j_1(x\sin(\theta/2))$, the MBA would lead to a simple formula for the prediction of the scatter size. The question of accuracy of the approximations in size determination will form the subject matter of a separate investigation.

Acknowledgments

The authors would like to thank Professor Swapan K Sen of the Saha Institute of Nuclear Physics and Professor Binayak Dutta-Roy at the S N Bose National Centre for Basic Sciences for constant encouragement and helpful discussions throughout the work.

References

[1] Waterman P C 1969 New formulation of acoustic scattering *J. Acoust. Soc. Am.* **45** 1417–29
[2] Morse P M and Ingard K U 1968 *Theoretical Acoustics* (New York: McGraw-Hill) chapter 8
[3] Saxon D S 1955 Lectures on the scattering of light *UCLA Department of Meteorological Science Report* no 9, University of California at Los Angeles, California
[4] Shimizu K 1983 Modification of Rayleigh–Debye approximation *J. Opt. Soc. Am.* **73** 504
[5] Perelman A Y 1991 Extinction and scattering by soft particles *Appl. Opt.* **30** 475–84
[6] Sharma S K and Somerford D J 1999 Scattering of light in the eikonal approximation *Prog. Opt.* **39** 311–90
[7] Glauber R J 1959 High energy collision theory *Lectures in Theoretical Physics* vol 1 ed W E Brittin and L G Dunham (New York: Interscience) pp 315–414
[8] Sharma S K and Somerford D J 1988 Modified Rayleigh–Gans–Debye approximation applied to sizing transparent homogeneous long fibres of intermediate size *J. Phys. D: Appl. Phys.* **21** 139–42
[9] van de Hulst H C 1957 *Light Scattering by Small Particles* (New york: Wiley)
[10] Gradshteyn I S and Ryzhik I M 1980 *Table of Integrals, Series and Products* (New York: Academic)
[11] Alvarez-Estrada R F, Calvo M L and del Egido Juncos 1980 Scattering of TM waves by dielectric fibres:Iterative and eikonal solutions *Opt. Acta* **27** 1367–78
[12] Perrin J M and Chiapetta P 1985 Light scattering by large particles: I. A new theoretical description of the eikonal picture *Opt. Acta* **32** 907–21